CHEMISTRY
A EUROPEAN JOURNAL

DOI: 10.1002/chem.200601250

Unusual Bond Formation in Aspartic Protease Inhibitors: A Theoretical Study

Julien Pilmé, Hélène Berthoumieux, Vincent Robert, and Paul Fleurat-Lessard*[a]

Abstract: The origin of the formation of the weak bond N|···C=O involved in an original class of aspartic protease inhibitors was investigated by means of the electron localization function (ELF) and explicitly correlated wavefunction (MRCI) analysis. The distance between the electrophilic C and the nucleophilic N centers appears to be controlled directly by the polarity and proticity of the medium. In light of these investigations, an unusual dative N−C bonding picture was characterized. Formation of this bond is driven by the enhancement of the ionic contribution C^+-O^- induced mainly by the polarization effect of the near N lone pair, and to a lesser extent by a weak charge delocalization N→CO. Although the main role of the solvating environment is to stabilize the ionic configuration, the protic solvent can enhance the C^+-O^- configuration through a slight but cumulative charge transfer towards water molecules in the short N−C distance regime. Our revisited bond scheme suggests the possible tuning of the N−CO interaction in the design of specific inhibitors.

Keywords: ab initio calculations · chemical bonding · density functional calculations · ELF (electron localization function) · protease inhibitors

Introduction

Understanding the nature of chemical bonding has always fascinated chemists.[1] Even though strong bonds are now well understood, the debate around the origin of weak bonds is always considerable, a prototype of such being the hydrogen bond.[2] In this context, the interaction of a tertiary amino-group nitrogen with a carbonyl double bond, that is, N|···C=O, has attracted much attention over several decades. This particular bond was first postulated by Kermack and Robinson to explain the low activity of the carbonyl group in the cryptopine and protopine alkaloids.[3] Later, it was seen in other alkaloids as a flexible ring clasp. Since then, this intriguing interaction has appeared in many areas of chemistry and biochemistry. In particular, it was used by Bürgi et al. to map the reaction coordinate of the nucleophilic addition to a carbonyl group.[4] It was also postulated in the challenging issue of the enantioselective heterogeneous hydrogenation of aldehydes, in which it links the CO moiety to the chiral modifier of the catalyst.[5] Because peptide bonds are the key to protein structure and activity, biological analogues based on this interaction can be anticipated.[6] Recently, the N|···C=O interaction was used as the central part of new candidates for inhibitors of aspartic proteases.[7] These enzymes are known to have key functions in the replication of the HIV virus and the development of Alzheimer's disease. The N|···C=O interaction is interesting as it should lead to inhibitors with not only steric but also electronic properties that mimic those of the transition-state structure. Indeed, the standard description of this bond involves a $N^{\delta+}-C-O^{\delta-}$ charge separation that closely mimics that arising during an amide-bond hydrolysis (Figure 1). Because this first candidate revealed a low inhibiting power ($IC_{50} > 1\,\mu mol$), one might wonder what the source (electronic or steric) of this deficiency might be. Therefore, a detailed understanding of this particular bond would be highly desirable in the design of this new class of inhibitors.

[a] Dr. J. Pilmé, H. Berthoumieux, Dr. V. Robert, Dr. P. Fleurat-Lessard
Laboratoire de Chimie, UMR CNRS 5182
Ecole Normale Supérieure de Lyon
46 Allée d'Italie, 69364 Lyon Cedex 07 (France)
Fax: (+33) 472-728-860
E-mail: Paul.Fleurat-Lessard@ens-lyon.fr

Supporting information for this article is available on the WWW under http://www.chemeurj.org/ or from the author: Table S1 lists the main structural parameters for the $Me_2N-(CH_2)_3-CH=O$ model system optimized at the B3LYP/6-31+G(d) level solvated by up to four water molecules with and without PCM; Table S2 gathers the distances and binding energies for the bimolecular system at different levels of calculation (see text); listing of cartesian coordinates for the main optimized structures (gas phase, PCM) obtained at the B3LYP/6-31+G(d) level; listing of cartesian coordinates at the 6-31+G* and aug-cc-pVTZ for the bimolecular test system $NMe_3|\cdots H_2CO$.

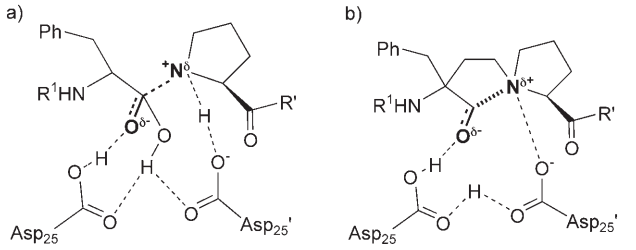

Figure 1. a) Transition state of the enzymatic reaction. b) Inhibitor candidate employing the N···CO bond.

Starting with the milestone studies of Leonard,[8] many experimental groups have investigated this interaction by using various techniques.[9–12] Surprisingly, the N–C distance is very sensitive to the environment (e.g., solvation effects),[12c] with variations between 1.6 and 2.9 Å being reported.[4,13] Experimental values are split into two groups, corresponding to a short-distance regime ($d_{CN} \leq 2.0$ Å) and a long-distance regime ($d_{CN} \geq 2.5$ Å). From the theoretical side, all parameterization using standard force fields have been unsuccessful so far.[6a,9d] Ad hoc empirical corrections were necessary to reproduce approximately molecular structures of cryptopine and clivorine, excluding any transferable parameters.[6a] This, added to the extreme variability of the bond length, may suggest a more subtle bonding picture than the traditional $n_N(\sigma\text{-donor}) \rightarrow \pi^*_{CO}(\text{acceptor})$ scheme.[8,9]

Considering the tremendous importance and unresolved character of this particular interaction, the purpose of the current work is to provide a further understanding of the intrinsic nature of this bond and to extract information on the relationship between the solvation effects and the observed distances regimes. Thus, a model system $Me_2N–(CH_2)_3–CH{=}O$ was chosen as a realistic candidate of amino aldehyde molecules[12c] to scrutinize the nature of the N|···C=O bond (Figure 2).

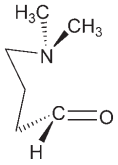

Figure 2. Model system of the tertiary amine–carbonyl bond.

In this context, one might wish to call for a detailed electronic description based on state-of-the-art calculations. The topological analysis of the electron localization function (ELF)[14] based on density functional theory (DFT) calculations appears as a natural and powerful tool to describe the chemical bond. In addition to the ELF analysis, explicitly correlated wave-function analysis obtained from ab initio multi reference configuration interaction (MRCI) calculations were also considered.

Computational Details

DFT calculations were performed by using the Gaussian 03 program.[15] The hybrid density functional B3LYP was used[16] with the standard basis set 6-31+G(d)[17] for all atoms. The diffuse functions are compulsory to correctly describe the ionic form of the carbonyl moiety. Comparative studies have been also carried out with the aug-cc-pVTZ basis sets.[18] Both basis sets display very similar results in the geometry optimizations. To validate the use of this particular functional, tests have been performed with BPW91[19] and MPWB1K[20] functionals. Furthermore, MP2 and CCSD(T) calculations were carried out to validate our DFT approach. The polarizable continuum model (PCM) of Tomasi et al.,[21] using the integral equation formalism, was used for calculations of the solvated model.

The binding energy (BE) values were corrected of the basis set superposition error (BSSE). As BE and BSSE are not easily accessed for an intramolecular bond, they were estimated by using the bimolecular test system $Me_3N|\cdots H_2CO$. By using the standard counterpoise correction,[22] BSSE was estimated to be 1.2 kcal mol^{-1} at the B3LYP/6-31+G(d) level.

By using the DFT optimized structures, we then performed MRCI wave-function analysis to investigate the contributions of polarization and charge-transfer effects. Complete active space self-consistent (CASSCF) simulations were performed by using the MOLCAS package, optimizing simultaneously the orbitals and the wave-function coefficients for a four-electron–three-molecular-orbital (MO) active space.[27] Dynamical correlation effects were then estimated by including single and double excitations in a variational procedure on top of the CASSCF wave function, as available in the CASDI code.[28] The Cowan–Griffin ab initio pseudopotential and basis sets of double zeta+diffuse+polarization quality were used on N (5s5p1d)→[2s3p1d], C (5s5p1d)→[2s3p1d], and O (5s6p1d)→[2s4p1d] atoms,[29] whilst H atoms were depicted with minimal basis set (STO-3G) [1s].[30] The CAS(4,3) validity was checked by including more active orbitals and electrons up to a CAS(8,7). The added orbitals remained either doubly occupied or vacant

Bonding Analysis

Two distinct approaches were considered for the bonding analysis. First, in addition to the DFT wave function, the ELF approach has been used extensively for the analysis of chemical bonding or chemical reactivity.[23] The relationship of the ELF function to pair functions has been demonstrated,[24] however, ELF values can be calculated more easily than the characteristics of pair functions. The ELF function can be interpreted as a signature of the electronic-pair distribution, split into an intuitive chemical picture: core- (labeled C(A)), bonding- (labeled V(A, B)), and nonbonding- (labeled V(A)) region pairs (the so-called basins). This is to be contrasted with the "atoms in molecules theory",[25] in which basins are localized on the atoms only. These ELF regions match closely the domains of the VSEPR model.[26] Therefore, the ELF analysis should enable us to follow the change in interaction nature. The basin (atomic or ELF) populations are calculated by integrating the charge density over the basin volume.

Second, the correlated wave function extracted from our MRCI calculations was analyzed in terms of the ionic, covalent, and charge-transfer components.

All the topological analyses were carried out from a Kohn–Sham wave function with the TopMoD[14c] package. The ELF and MO isosurfaces were visualized by using the Molekel[31] software.

Results and Discussion

B3LYP calculations of our model system lead us to the qualitative and nonambiguous conclusion that the N–C distance appears clearly controlled by environmental effects. Indeed, in the gas phase, the DFT optimization of our model system exhibits rather long N–C (2.86 Å) and short C–O (1.22 Å) distances (see Table S1 in the Supporting Information). Mimicking the physiological medium by using a polarizable continuum model (PCM with $\varepsilon_r = 78.4$) shortens the N–C distance to 2.54 Å. Nevertheless, such a value is much larger than the typical N–C experimental distances observed in amino ketone derivatives.[12c] This result strongly suggests that one has to take into account explicitly the protic character of the medium. Indeed, calculations using an embedding continuum ($\varepsilon_r = 78.4$) together with a single water molecule to account explicitly for the protic character of the solvent exhibit a drastic shortening of the N–C distance (1.81 Å). This single result supports the stabilizing effect of the protic environment favoring the short-distance regime. Simultaneously, unusually long C–O distances (see Table S1 in the Supporting Information) and significant pyramidalization of the carbon atom (>30% sp^3 character) are observed. This is to be contrasted with the Bürgi–Dunitz NCO angle[4] that remains close to 110° for all N–C distances. These structural effects are related to an increase in the binding energy from 2 kcal mol^{-1} (gas phase) to 9 kcal mol^{-1} (PCM and one water molecule), that is, twice the average hydrogen-bond value.

To confirm this trend, several additional calculations were performed by using other methods (BPW91, MPWB1K, and MP2) with 6-31+G(d) and aug-cc-pVTZ basis sets for the bimolecular model system $NMe_3|\cdots H_2CO$. The main results (distances and binding energies) are presented in Table S2 in the Supporting Information and reveal qualitatively similar results: upon addition of one water molecule and a continuum, the system switches from the long-distance regime (>2.5 Å) to the short-distance regime (<2.0 Å), together with a significant increase in the binding energy. These conclusions were confirmed by a reference CCSD(T) optimization of the bimolecular system with one water molecule embedded in a continuum: $d_{CN} = 1.653$ Å, BE = 11 kcal mol^{-1} (BSSE corrected), compared to B3LYP values $d_{CN} = 1.715$ Å and BE = 9 kcal mol^{-1} (BSSE corrected). All of these calculated parameters are in excellent accord with experimental studies.[4,13]

To understand the role of the environment, we then conducted some calculations by using different models. Previous theoretical studies have shown that the first solvation shell of the carbonyl-O lone pairs consists of two to three water molecules. This is to be contrasted with the environment of the hydroxide ion HO^-, which involves up to four water molecules.[32] Thus, we carried out calculations of our system in the presence of three or four water molecules. In each case, we also tested the effect of adding an embedding PCM, leading to four calculations. All optimized structures display short N–C distances (from 1.87 to 1.63 Å) and quite large C–O distances (from 1.25 to 1.34 Å), whatever the environment (see Table S1 in the Supporting Information). Furthermore, convergence of the critical N–C distance is achieved (variation ≈2%) for an environment consisting of four water molecules with PCM. However, as the number of water molecules is increased, the effect of the PCM embedding is reduced. With four water molecules, the difference between the N–C distances of the two models (gas phase and PCM) is smaller (0.06 Å) than the dispersion observed experimentally[4,12,13] in the short regime (0.20 Å). Thus, to analyze the bonding properties, we felt that the inclusion of only four explicit water molecules would be a reasonable model to describe both the polar and protic effects of the solvating environment (see Figure 3).

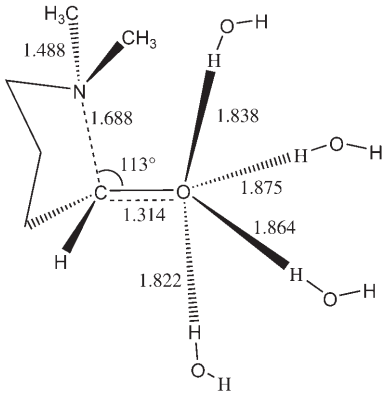

Figure 3. Model system in the presence of four water molecules. The distances [Å] and the Bürgi–Dunitz NCO angle [°] are given for the optimized B3LYP/6-31+G(d) calculation without PCM.

At this stage, the fundamental question of the intrinsic electronic nature of the intramolecular NCO bond in the two regimes deserves special attention. As our aim was to unravel the nature of the NCO interaction, we selected five N–C distances representative of the long-distance regime ($d_{CN} = 3.0$ Å) and of the short-distance regime ($d_{CN} = 1.90$, 1.81, 1.70, and 1.63 Å, Table 1). This set of distances allows us to cover the experimental range of N–C distances observed for different compounds,[4,12] as well as optimized values obtained with various computational approaches. For each selected distance, partial geometry optimizations were carried out both in the gas phase for the model system (see Figure 2) alone and in the presence of four water molecules (see Figure 3), the C–N distance remaining constant.

We then performed ELF analysis of the DFT wave function for both model systems. Explicitly correlated MRCI wave-function analysis (CASSCF+singles and doubles CI) were conducted to validate the conclusions of the ELF analysis. Such a strategy allows one to concentrate on the intimate nature of this interaction as a function of structural parameters controlled by environmental effects. Figure 4 displays the ELF localization domains of the model system for two typical N–C distances (1.81 and 3.0 Å).

Table 1. C–O bond length, ELF population, and correlated wave-function analysis for the optimized gas-phase model system for five selected N–C distances. The values given in parenthesis were calculated in the presence of four water molecules solvating the carbonyl group.

d_{CN} [Å][a]	3.00	1.90	1.81	1.70	1.63
			CO bond-length evolution		
d_{CO} [Å]	1.21 (1.23)	1.25 (1.28)	1.26 (1.30)	1.27 (1.31)	1.28 (1.32)
			ELF population analysis		
$\bar{N}V(O)$[b]	5.21 (5.26)	5.64 (5.70)	5.73 (5.85)	5.87 (5.94)	5.95 (6.03)
$\bar{N}V(C,O)$[c]	2.38 (2.30)	2.05 (1.89)	1.94 (1.73)	1.82 (1.63)	1.71 (1.55)
$\delta q_{N\rightarrow CO}$[d]	0(0)	0.1(0.1)	0.12(0.13)	0.14(0.15)	0.18(0.19)
			Correlated wave-function analysis		
% ionic	34	49	53	58	67
C–O/N–C[e]	>60	4.30	2.92	2.06	1.95

[a] Frozen during the optimization. [b] Oxygen lone-pair population [c] C–O bonding population. [d] Relative net charge transfer N→CO calculated with the atomic populations.[16] [e] Covalent ratio (see text and ref. [35]).

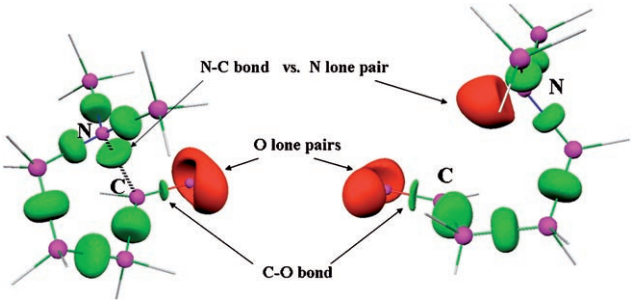

Figure 4. ELF localization domains (protonated bonds have been omitted for clarity) of the tertiary amine–carbonyl model system for two typical distances: left) $d_{CN}=1.81$ Å, right) $d_{CN}=3.0$ Å. Color code: magenta: core; red: nonbonding; green: bonding.

As illustrated in Figure 4, the pure nitrogen lone pair is observed at large N–C distances. There is no covalent interaction with the carbonyl moiety, suggesting a weak Van der Waals bond. Conversely, as the N–C distance shortens, the lone pair becomes progressively involved in a partially dative N–C bond, as one may expect.[19] However, the calculated bonding basin is still centered close to the nitrogen atom and, interestingly, only a small contribution of the carbon atomic domain to the bonding population is observed (16% at $d_{CN}=1.63$ Å). This is much smaller than in a typical covalent peptide bond, such as Me_2N–CH=O, in which this contribution reaches up to 40%. Thus, our ELF analysis of the model system (Figure 2) supports a weak covalent character for the N–C interaction as opposed to the well-known scenario $n_N\rightarrow\pi^*_{CO}$. Let us stress that the global charge transfer from nitrogen towards the carbonyl fragment is positive, but rather small ($\leq$0.19 e). This is to be compared with the protonated system $Me_2N(CH_2)_3$–C^+H–OH in which the equilibrium C–N distance equals 1.58 Å, and the charge transfer is 50% larger (0.27 e). Meanwhile, the carbonyl moiety undergoes deep charge reorganization under the polarizing effect of the N lone pair. As seen in Table 1, a simultaneous increase in the oxygen lone pair (5.21 e→5.95 e) and reduction in the C–O bond populations (2.38 e→1.71 e) are to be noticed along formation of the N–C bond. Therefore, the ELF population analysis of the model system sheds new light on the nature of the N|···C=O interaction, which, in our view, should be described as an enhancement of the ionic character of the C–O bond as the N–C distance decreases, ruling out the traditional N^+–C–O^- picture resulting from the density transfer $n_N\rightarrow\pi^*_{CO}$.[8,9]

At this stage, one can easily grasp why solvation plays such a role in determining the distance regime: a polar medium is needed to stabilize the ionic form. However, to fully clarify the influence of the water molecules, we performed an ELF population analysis of our system surrounded by four water molecules (Table 1). The populations of the O lone pair and N–C bond are affected mainly by the vicinity of the N atom, regardless of the presence of water molecules. Indeed, valence population changes induced by the addition of the water molecules are five times smaller than those due to shortening of the N–C bond (Table 1). This shows that the first role of the solvent is to stabilize the charge separation. As a consequence, the electronic distribution on the Me_2N–$(CH_2)_3$–CH=O moiety does not depend upon the presence of the water molecules. This in turn fully supports our previous conclusion that the solvated NCO interaction is best described as [N|C=O↔N|···C^+–O^-]. On top of this main effect, a very small net charge transfer (0.04 e) is observed from the CO bond to each water molecule at $d_{CN}=1.63$ Å. By cumulative effect, the C–O bond is depopulated (1.71 e→1.55 e), which induces a destabilization of the C–O covalent bond and consequently, an increase in the C–O distance. Finally, this analysis shows that the protic environment is able to enhance slightly the C^+–O^- configuration in addition to its main electrostatic stabilizing role.

Our previous ELF analysis confirmed that the main role of the medium is essentially electrostatic, the electronic distribution of the model system being very similar, whatever the protic environment. Consequently, MRCI calculations, using the DFT geometries, were conducted only on the model system of Figure 2. The particular splitting into ionic and covalent contributions is accessible directly from explicitly correlated methods that are very insightful into the analysis of bond-formation phenomena. Large configuration interaction (CI) calculations have been used with great success in the study of electronic properties of molecular and solid-state materials.[33] It has been reported that DFT tends to systematically exaggerate delocalization effects,[34] whereas CI approaches account accurately for subtle charge-reorganizations processes. Thus, with the goal of microscopic interpretation in mind, we felt that state-of-the-art ab initio calculations would be complementary to our combined DFT/ELF analysis. A complete active-space (four electrons/three orbitals) self-consistent field method was used to generate MOs for our subsequent correlation calculations, including single and double excitations. The speculated bond-formation mechanism $n_N\rightarrow\pi^*_{CO}$ suggests the active participation

of the N lone pair and the frontier orbitals of the carbonyl fragment, which are very similar to the π_{CO} and π^*_{CO} MOs (Figure 5).

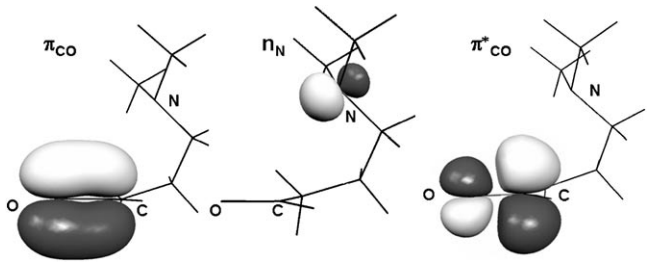

Figure 5. Frontier MOs of the tertiary amine–carbonyl model system.

These frontier MOs were relocalized on the C and O centers to grasp the charge reorganization in a valence-bond-type analysis. In agreement with the small charge transfer found in our ELF analysis ($\delta q_{N\rightarrow CO} \leq 0.18$), the n_N orbital remains almost doubly occupied (at least 1.997 e), excluding any significant $n_N \rightarrow \pi^*_{CO}$ mechanism. The correlated wave function (see Table 1) is dominated by the ionic contributions (i.e., C^+O^- and C^-O^+) at the short-distance regimes ($d_{CN} \leq 1.90$ Å). As for the covalent part, the participation of the carbon atom was analyzed by using the ratio of the covalent contributions[35] of the C–O and N–C bonds. Even though bond formation is strongly suggestive of a four-electron/three-center scheme, the remarkable feature is a significant reduction (60→1.95, Table 1) of this covalent-contribution ratio: as the C–N distance decreases, the carbon covalent participation is partly redirected from the CO bond to the forming CN bond. This in turn seems to be a determining process. In addition, this analysis of the correlated wave function confirms the nondispersive character of the N–C–O bond. Let us stress that the validity of the DFT approach is thus demonstrated a posteriori.

Conclusion

The nature of the N|···CO interaction was reconsidered extensively on the basis of combined ELF analysis and ab initio calculations. Our ELF topological analysis differentiates clearly the long and short N–C distance regimes. The four-electron/three-center picture that has been conveyed so far in the literature suffers from the absence of any strong $n_N \rightarrow \pi^*_{CO}$ charge transfer. From our point of view, the bond formation is driven clearly by the enhancement of the ionic contribution C^+–O^- induced by the strong polarization effect of the near N lone pair. Conversely, the covalent character of the CN bond is still much weaker ($\approx$1/3) than that of the CO bond. Our results obtained by including water molecules validate the N|···C^+–O^- bonding scheme and clarify the fundamental role of the solvating environment, which stabilizes mainly the ionic C^+–O^- configuration, but also enhances this configuration at the very short-distance regimes. A suitable parameterization for such nondispersive interaction necessarily relies on a high-level description of the intimate intramolecular-charge reorganization. Our work supports strongly the role of the medium, whose effects can be theoretically tuned to account for the crucial water-excluding folding processes of biological systems. Finally, our results provide a revisited scheme for the N|···CO interaction. Thus, we hope that this bonding scheme will assist in the synthesis of more-efficient inhibitors.

[1] G. N. Lewis, *J. Am. Chem. Soc.* **1916**, *38*, 762.
[2] M. E. Tuckerman, D. Marx, M. L. Klein, M. Parrinello, *Science* **1997**, *275*, 817; S. B. Suh, J. C. Kim, Y. C. Choi, S. Yun, K. S. Kim, *J. Am. Chem. Soc.* **2004**, *126*, 2186.
[3] W. O. Kermack, R. J. Robinson, *J. Chem. Soc. Trans.* **1922**, *121*, 427.
[4] H. B. Bürgi, J. D. Dunitz, E. Schefter, *J. Am. Chem. Soc.* **1973**, *95*, 5065; H. B. Bürgi, J. D. Dunitz, E. Schefter, *Nature New Biol.* **1973**, *244*, 186; H. B. Bürgi, J. D. Dunitz, *Acc. Chem. Res.* **1983**, *16*, 153.
[5] J. W. de M. Carneiro, C. da S. B. de Oliveira, F. B. Passos, D. A. G. Aranda, P. Rogério N. de Souza, O. A. C. Antunes, *J. Mol. Catal. A* **2001**, *170*, 235; M. Studer, H.-U. Blaser, C. Exner, *Adv. Synth. Catal.* **2003**, *345*, 45.
[6] a) R. Griffith, J. B. Bremner, S. J. Titmuss, *J. Comput. Chem.* **1997**, *18*, 1211; b) R. Griffith, B. F. Yates, J. B. Bremner, S. J. Titmuss, *J. Mol. Graph. Model.* **1997**, *15*, 91; c) R. Griffith, J. B. Bremner, *J. Comput.-Aided Mol. Des.* **1999**, *13*, 69.
[7] A. Gautier, D. Pitrat, J. Hasserodt, *Bioorg. Med. Chem.* **2006**, *14*, 3835.
[8] a) N. J. Leonard, *Rec. Chem. Prog.* **1956**, *17*, 243, and references therein; N. J. Leonard, *Acc. Chem. Res.* **1979**, *12*, 423, and references therein.
[9] a) G. Spanka, P. Rademacher, *J. Org. Chem.* **1986**, *51*, 592; b) G. Spanka, P. Rademacher, H. Duddeck, *J. Chem. Soc. Perkin Trans. 2* **1988**, 2119; c) P. Rademacher, *Chem. Soc. Rev.* **1995**, 143; d) G. Spanka, R. Boese, P. Rademacher, *J. Org. Chem.* **1987**, *52*, 3362.
[10] M. R. Bell, S. Archer, *J. Am. Chem. Soc.* **1960**, *82*, 151; M. R. Bell, S. Archer, *J. Am. Chem. Soc.* **1960**, *82*, 4638.
[11] R. McCrindle, A. J. McAlees, *J. Chem. Soc. Chem. Commun.* **1983**, 61.
[12] a) A. J. Kirby, I. V. Komarov, N. Feeder, *J. Chem. Soc. Perkin Trans. 2* **2001**, 522; b) A. J. Kirby, I. V. Komarov, V. A. Bilenko, J. E. Davies, J. M. Rawson, *Chem. Commun.* **2002**, 2106; c) J. E. Davies, A. J. Kirby, I. V. Komarov, *Helv. Chim. Acta* **2003**, *86*, 1222.
[13] a) S. R. Hall, F. R. Ahmed, *Acta Cryst. B* **1968**, *24*, 337; S. R. Hall, F. R. Ahmed, *Acta Cryst. B* **1968**, *24*, 346; b) J. A. Wunderlich, *Acta Cryst.* **1967**, *23*, 846; c) G. I. Birnbaum, *J. Am. Chem. Soc.* **1974**, *96*, 6165.
[14] a) A. D. Becke, K. E. Edgecombe, *J. Chem. Phys.* **1990**, *92*, 5397; b) B. Silvi, A. Savin, *Nature* **1994**, *371*, 683; c) S. Noury, X. Krokidis, F. Fuster, B. Silvi, *Comput. Chem.* **1999**, *23*, 597.
[15] Gaussian 03, Revision D.01, M. J. Frisch, G. W. Trucks, H. B. Schlegel, G. E. Scuseria, M. A. Robb, J. R. Cheeseman, J. A. Montgomery, Jr., T. Vreven, K. N. Kudin, J. C. Burant, J. M. Millam, S. S. Iyengar, J. Tomasi, V. Barone, B. Mennucci, M. Cossi, G. Scalmani, N. Rega, G. A. Petersson, H. Nakatsuji, M. Hada, M. Ehara, K. Toyota, R. Fukuda, J. Hasegawa, M. Ishida, T. Nakajima, Y. Honda, O. Kitao, H. Nakai, M. Klene, X. Li, J. E. Knox, H. P. Hratchian, J. B. Cross, V. Bakken, C. Adamo, J. Jaramillo, R. Gomperts, R. E. Stratmann, O. Yazyev, A. J. Austin, R. Cammi, C. Pomelli, J. W. Ochterski, P. Y. Ayala, K. Morokuma, G. A. Voth, P. Salvador, J. J. Dannenberg, V. G. Zakrzewski, S. Dapprich, A. D. Daniels, M. C. Strain, O. Farkas, D. K. Malick, A. D. Rabuck, K. Raghavachari, J. B. Foresman, J. V. Ortiz, Q. Cui, A. G. Baboul, S. Clifford, J. Cioslowski, B. B. Stefanov, G. Liu, A. Liashenko, P. Piskorz, I. Komaromi, R. L. Martin, D. J. Fox, T. Keith, M. A. Al-Laham, C. Y. Peng, A. Nanayakkara, M. Challacombe, P. M. W. Gill, B. Johnson, W.

Chen, M. W. Wong, C. Gonzalez, and J. A. Pople, Gaussian, Inc., Wallingford CT, **2004**.
[16] a) C. Lee, W. Yang, R. G. Parr, *Phys. Rev. B* **1988**, *37*, 785; b) A. D. Becke, *J. Chem. Phys.* **1993**, *98*, 5648.
[17] P. C. Hariharan, J. A. Pople, *Theor. Chim. Acta* **1973**, *28*, 213; T. Clark, J. Chandrasekhar, G. W. Spitznagel, P. von R. Schleyer, *J. Comput. Chem.* **1983**, *4*, 294.
[18] a) T. H. Dunning, Jr., *J. Chem. Phys.* **1989**, *90*, 1007; b) R. A. Kendal, T. H. Dunning, Jr., R. J. Harrison, *J. Chem. Phys.* **1992**, *96*, 6796.
[19] A. D. Becke, *Phys. Rev. A* **1988**, *38*, 3098; J. P. Perdew, Y. Wang, *Phys. Rev. B* **1992**, *45*, 13244.
[20] Y. Zhao, D. G. Truhlar, *J. Phys. Chem. A* **2004**, *108*, 6908.
[21] M. T. Cancès, B. Mennucci, J. Tomasi, *J. Chem. Phys.* **1997**, *107*, 3032; M. Cossi, G. Scalmani, N. Rega, V. Barone, *J. Chem. Phys.* **2002**, *117*, 43.
[22] S. F. Boys, F. Bernardi, *Mol. Phys.* **1970**, *19*, 553.
[23] a) X. Krokidis, S. Noury, B. Silvi, *J. Phys. Chem. A* **1997**, *101*, 7277; b) J. Pilme, B. Silvi, E. A. Alikhani, *J. Phys. Chem. A* **2005**, *109*, 10028; c) I. Fourré, B. Silvi, P. Chaquin, A. Sevin, *J. Comput. Chem.* **1999**, *20*, 897.
[24] B. Silvi, *J. Phys. Chem. A* **2003**, *107*, 3081.
[25] R. F. W. Bader, *Atoms in Molecules: A Quantum Theory*, Oxford University Press, Oxford, **1990**.
[26] R. J. Gillespie, R. S. Nyholm, *Q. Rev. Chem. Soc.* **1957**, *11*, 339.
[27] K. Anderson, M. P. Fluscher, G. Karlstrm, R. Lindh, P. A. Malqvist, J. Olsen, B. Roos, A. J. Sadlej, M. R. A. Blomberg, P. E. M. Siegbahn, V. Kello, J. Noga, M. Urban, P. O. Widmark, *MOLCAS*, *Version 5.4*, *University of Lund*, *Lund* (Sweden).
[28] N. Ben Amor, D. Maynau, *Chem. Phys. Lett.* **1998**, *286*, 211.
[29] Z. Barandiaran, L. Seijo, *Can. J. Chem.* **1992**, *70*, 409.
[30] W. J. Hehre, R. F. Stewart, J. A. Pople, *J. Chem. Phys.* **1969**, *51*, 2657.
[31] P. Flukiner, H. P. Luthi, S. Portman, J. Weber, *Molekel*, Swiss Center for Scientific Computing, Switzerland, **2000–2002**.
[32] a) S. Chalmet, M. F. Ruiz-Lopez, *J. Chem. Phys.* **1999**, *111*, 1117; b) T. Ishida, P. J. Rossky, E. W. Castner, Jr., *J. Phys. Chem. B* **2004**, *108*, 17585; c) A. Botti, F. Bruni, S. Imberti, M. A. Ricci, A. K. Soper, *J. Mol. Liquids* **2005**, *117*, 81; d) J. Pilmé, P. Fleurat-Lessard, unpublished results.
[33] C. J. Calzado, J. Cabrero, J.-P. Malrieu, R. Caballol, *J. Chem. Phys.* **2002**, *116*, 2728; C. J. Calzado, J. Cabrero, J.-P. Malrieu, R. Caballol, *J. Chem. Phys.* **2002**, *116*, 3985.
[34] J. Cabrero, C. J. Calzado, D. Maynau, R. Caballol, J.-P. Malrieu, *J. Phys. Chem. A* **2002**, *106*, 8146.
[35] By using the correlated wave function on the basis of localized orbitals, one can split the wave function into covalent and ionic (i.e., charge transfers $N^-C^+O^-$,N^+C^-O) contributions.

Received: August 31, 2006
Revised: December 20, 2006
Published online: March 27, 2007

